JOURNAL OF MATERIALS SCIENCE 23 (1988) 1164–1170

Surface crystallization in melt-spun metallic glasses

M. A. GIBSON, G. W. DELAMORE
Department of Metallurgy and Materials Engineering, University of Wollongong, P.O. Box 1144, Wollongong, New South Wales 2500, Australia

A series of hypoeutectic FeSiB metallic glasses produced by single-roller melt spinning were found to have substantial wheel-side surface crystallization. These crystals were shown to be associated with areas on the ribbon surface which were in good contact with the wheel rather than in the depressions formed by gas entrainment during casting, as has been previously suggested for similar effects in other alloys. Transmission electron microscopy revealed that the crystals have a fine cellular substructure with the intercellular spaces freezing as glass and that the structure becomes progressively finer during growth.

1. Introduction

There have been several reports of surface crystallization in otherwise glassy ribbons produced by the various forms of melt spinning [1–5]. In most cases these crystals have been found at the free surface of the ribbons, i.e. that surface not in contact with the wheel in single-roller melt spinning, and the presence of such crystals has been explained in terms of the lower cooling rate at this surface. There have also been isolated reports of wheel-side crystallization which are difficult to explain by arguments based on reduced cooling rates. Davis *et al.* [1] found evidence of wheel-side crystallization in ribbons of Metglas 2605S ($Fe_{82}B_{12}Si_6$), and concluded that this was due to oxidation of boron by air trapped between the melt puddle and the wheel surface during the spinning operation. The depressions formed on the wheel-side surface of the ribbons resulting from this gas entrapment were believed to be nucleation sites for the surface crystals which form because of the shift in melt composition outside the easy glass-forming range coupled with the lower cooling rate in the depressions due to their lack of direct contact with the wheel surface. Similar surface crystallization was reported by Choi *et al.* [4] on ribbons of Metglas 2605 CO ($Fe_{67}Co_{18}B_{14}Si_1$), although they were unable to detect any compositional variation between the gas pocket depressions and the remainder of the ribbon surface and, like Davis, they did not positively identify the position of the nucleation sites on the ribbon surface. Jones *et al.* [5] confirmed these findings in Metglas 2605 CO but they too were unable to offer any explanation for their formation on the wheel-side of the ribbons. Fredriksson *et al.* [6] reported surface crystals with a distinctly dendritic morphology on the wheel-side of ribbons of FeNiPB alloys and developed simple heat transfer/crystal growth-rate models to account for the crystal-to-glass transition during solidification. They concluded that, following nucleation, the crystal growth rate at first increases rapidly and then decreases, despite the fact that the melt temperature ahead of the interface is predicted to fall continuously, and suggested that the transition occurred when the growth rate of the crystals fell to zero. Massalski and co-workers [7, 8] have also analysed the conditions for nucleation and growth of crystals during rapid freezing and the competition between crystallization and glass formation. They concluded that a crystal-to-glass transition is possible during solidification if the velocity with which the isotherms traverse the melt puddle is greater than the velocity of the crystal–melt interface.

The work presented here is part of a wider study of crystallization of iron-based metallic glasses. It was found that many hypoeutectic FeSiB alloys showed evidence of wheel-side crystallization with features different from those previously reported.

2. Experimental procedure

A series of FeSiB alloys with total metalloid content varying from 18 to 22 at. % were prepared from high-purity components. The constituents were alloyed in sealed quartz tubes in a reduced argon atmosphere and the alloy buttons subsequently homogenized by remelting several times on the water-cooled hearth of an arc furnace. Ribbons 5 mm wide and 15 to 30 μm thick were melt-spun in air using the planar flow casting technique on a 30 cm diameter stainless steel wheel rotating at 2500 r.p.m.

The as-cast ribbons were examined by X-ray diffraction on each surface and metallographically on unprepared surfaces and mounted cross-sections. Specimens were heat treated both in a Mettler TA 3000 differential scanning calorimeter and also, for larger samples, in a tin bath. The morphology and identity of the crystallization products were examined by transmission electron microscopy. Foils were prepared in a Struers Tenupol twin-jet polisher, the wheel-side surface being masked so that polishing occurred exclusively from the free surface.

0022–2461/88 $03.00 + .12 © *1988 Chapman and Hall Ltd.*

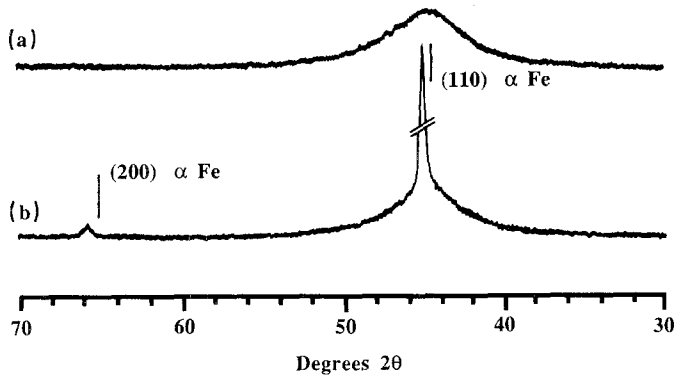

Figure 1 X-ray diffraction traces from (a) the free surface and (b) the wheelside surface of an $Fe_{80}Si_{10}B_{10}$ alloy ribbon. Markers indicate the expected peak positions for pure iron.

3. Results

3.1. As-cast alloys

X-ray diffraction traces from both surfaces of $Fe_{80}Si_{10}B_{10}$, which are typical of all the alloys examined, are presented in Fig. 1 which indicates that only the substrate surfaces of each of the ribbons showed some evidence of crystallinity. Compositions close to the glass-forming boundary [9] – in general those with a lower total metalloid content – were apparently more susceptible to surface crystallization as evidenced by a significant increase in the height of the X-ray diffraction peak from these alloys.

Optical metallography of the etched but otherwise unprepared ribbon surfaces confirmed these observations. Fig. 2 shows that the substrate surfaces are covered with small, circular crystalline regions which are larger and cover a greater area of the surface as the alloy composition decreases in metalloid content. It is apparent that these regions are not randomly distributed over the substrate surface but tend to decorate the ridges on the ribbon surface, Figs 2c and 3b, which result from grinding marks left on the wheel during preparation. There was no evidence of nucleation within the gas-pocket depressions but once nucleated elsewhere, crystals were found to grow into these areas.

Optical metallography of ribbon cross-sections (Figs 3a and c) showed that the crystals invariably nucleate at the wheel–ribbon interface and advance into the melt with hemispherical growth fronts: there was no evidence of nucleation within the bulk of the liquid. The crystals appeared structureless at optical microscopy magnifications but transmission electron microscopy of the as-cast specimens revealed that the crystals have a very fine, barely resolvable cellular substructure (Fig. 4). There are also larger-scale areas of contrast within the crystals which are due to slight misorientations in alignment during growth, as the bright-field/dark-field photographic pairs shown in Fig. 5 indicate. The interface between the glass matrix and the crystals is relatively sharp, but it was not possible to distinguish its precise shape because of the fineness of the structure. A significant feature of the substructure within the crystals is that the cell

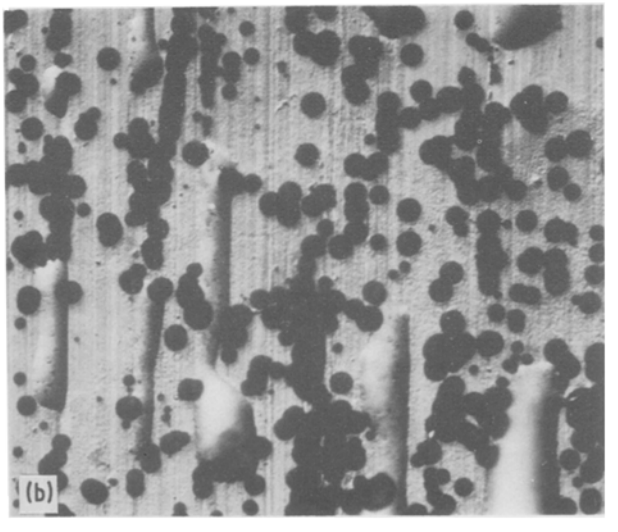

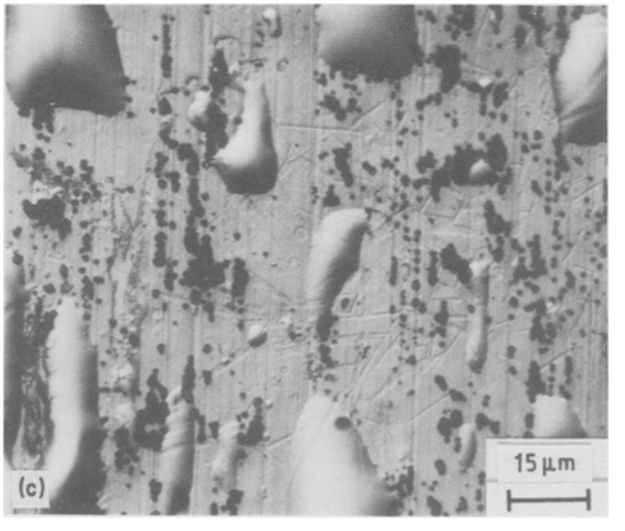

Figure 2 As-cast wheel-side surfaces of (a) $Fe_{82}Si_8B_{10}$, (b) $Fe_{80}Si_{10}B_{10}$ and (c) $Fe_{78}Si_{12}B_{10}$ ribbons showing the extent of substrate crystallization. Sodium metabisulphite etch.

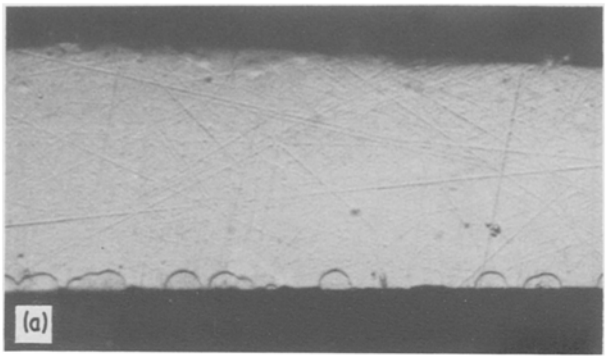

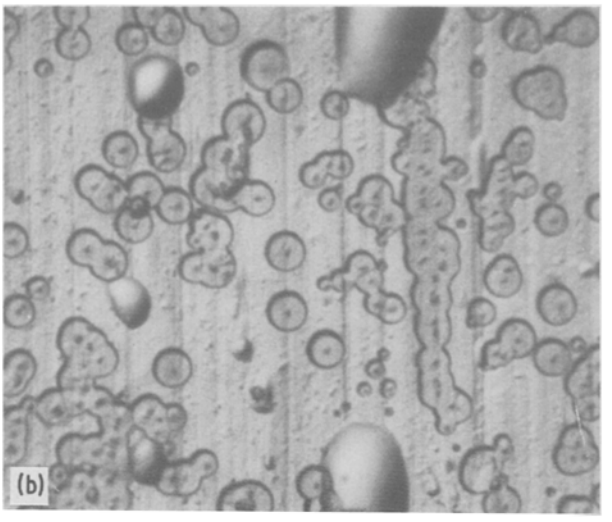

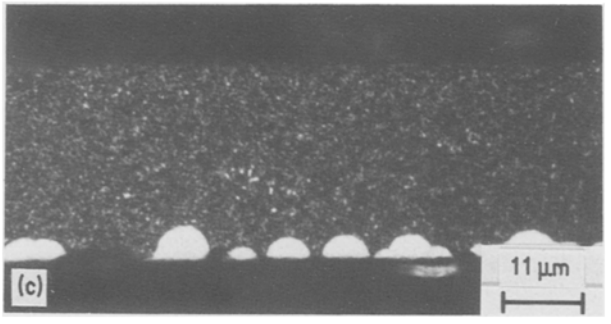

Figure 3 $Fe_{80}Si_{10}B_{10}$ ribbons. Nital etch. (a) As-cast cross-section showing hemispherical growth fronts of substrate crystals. (b) As-cast surface showing alignment of crystals with wheel grinding marks. (c) Fully crystallized ribbon cross-section.

dimensions decrease during growth, i.e. the structure becomes progressively finer from the centre towards the crystal–glass interface, as Fig. 6 shows.

Electron diffraction patterns taken from individual crystals gave single-crystal patterns which were indexed as originating from a bcc cell of dimensions $a = 0.2830$ nm, in agreement with the X-ray diffraction data. In addition to the bcc reflections, the pattern also contained diffuse rings (Fig. 5d) with a spacing which matched exactly those in patterns taken from the glassy matrix. Dark-field images taken from these rings highlight the intercellular regions in the crystal (Fig. 5c).

3.2. Heat-treated alloys

All the alloys examined in this work crystallize on heating by a two-stage process, in common with most hypoeutectic alloys in the FeSiB system [10, 11]. The first stage involves crystallization of iron-rich dendrites, followed at a higher temperature by transformation of the residual glassy matrix via a eutectic reaction. On heating the ribbons to a temperature equivalent to the first stage of crystallization, the substrate crystals developed dendritic perturbations at the crystal–glass interface while the amorphous matrix partially transformed by the nucleation and growth of α-Fe dendrites (Fig. 7a). Although it was not possible to detect any structural change in the interior of the substrate crystals, electron diffraction patterns showed that their lattice parameter had increased to 0.2868 nm, the same value as that of the newly formed dendrites in the matrix. The diffuse rings found in the as-cast pattern were still present after this low-

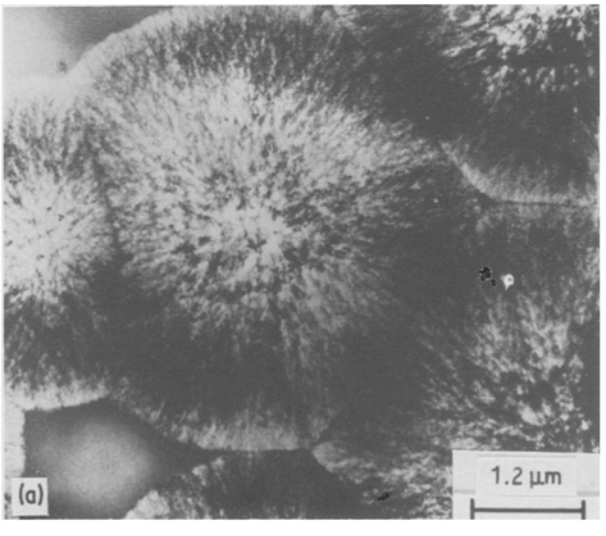

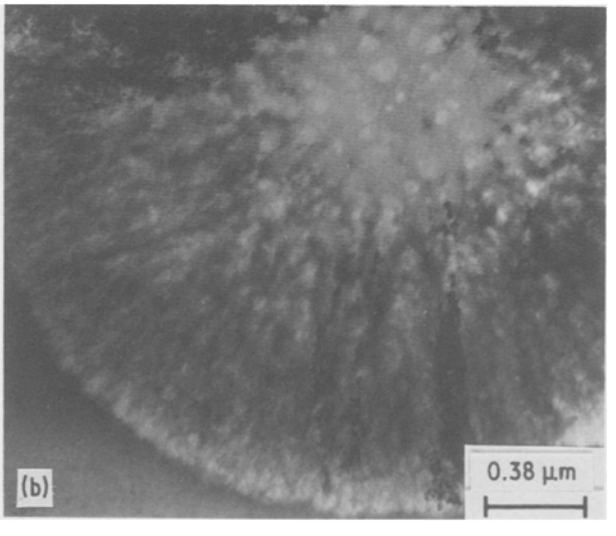

Figure 4 Transmission electron photomicrographs of crystals in $Fe_{80}Si_{10}B_{10}$. The crystals have a very fine substructure and a sharp interface with the glassy matrix.

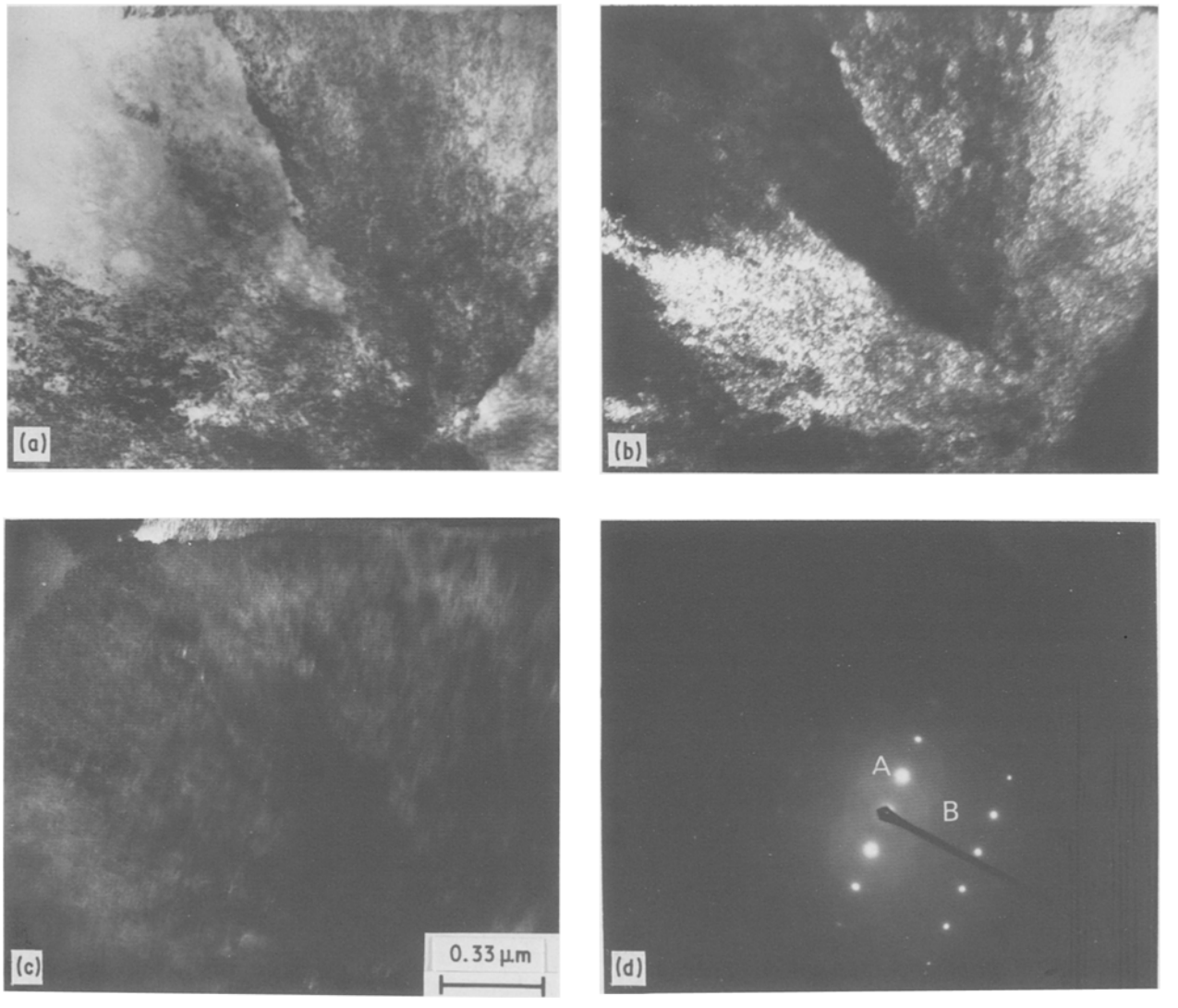

Figure 5 (a) Bright-field photomicrograph of a crystal in $Fe_{82}Si_8B_{10}$. (b) Dark-field image from spot A showing areas of slight misorientation in the crystal. (c) Dark-field image from ring B, highlighting intercellular regions. (d) Electron diffraction pattern from the crystal.

temperature heat treatment (Fig. 7c), but were replaced by numerous diffraction spots, as shown in Fig. 7d, when completely crystallized by heating to higher temperatures.

4. Discussion

The results of this work show clearly that suggestions that surface crystallization is associated with regions of low cooling rate on the wheel surface are inappropriate in this case. On the contrary, there is a tendency for crystals to nucleate at positions on the melt–wheel interface which are regions of high cooling rate. Biloni and Chalmers [12] in their early work on the formation of predendritic regions in chill-cast aluminium copper alloys also found that nucleation occurred preferentially at the mould–metal interface at grinding marks left on the mould surface. They argued that these surface grooves were regions of high heat removal rate because of their geometry and may also have been favourable sites for nucleation. The fact that in the present work also all the crystals were found to nucleate exactly at the wheel–melt interface rather than within the bulk liquid suggests that the wheel surface is providing heterogeneous nucleation sites rather than simply a high cooling rate: all parts of the melt puddle which subsequently solidify as glass must have cooled to temperatures well below the nucleation temperature, T_n, and therefore avoided crystallization only because of the lack of suitable nucleation sites.

Although Biloni and Chalmers showed that the predendritic stages of growth in their surface crystals were partitionless, the fine substructure of the surface crystals in this work is clearly two-phase as shown by the electron diffraction patterns. The diffuse rings superimposed on the single-crystal pattern (Fig. 5d) suggest that the intercellular regions are amorphous as reported by Adam [13] for similar structures (described by him as microeutectic), in AlFeMo alloys. Interdendritic glass has also been reported by Boettinger in unidirectionally grown PdCuSi alloys [14] and by Kelly and VanderSande in rapidly-quenched steels [15]. Boettinger *et al.* [16] were also able to show that the intercellular regions in rapidly solidified AlFe alloys contained fine crystals which they suggested resulted from precipitation from an originally amorphous phase. The replacement of the ring pattern by spots when the ribbons are fully crystallized (Fig. 7d) suggests strongly that the intercellular regions in our work were originally glassy rather than microcrystalline.

Figure 6 Transmission electron photomicrograph of a crystal in $Fe_{82}Si_8B_{10}$ showing progressive refinement of the substructure during growth from the crystal centre (top) to the outside (bottom).

Comparison of the lattice spacings of the crystals in the as-cast and heat-treated conditions indicates that they are supersaturated with boron during growth – both boron and silicon in solution in iron reduce its lattice parameter [17, 18]. On heating the as-quenched ribbons into the first stage of transformation, the lattice parameter of the substrate crystals increases towards the value for essentially pure iron, identical with values obtained from the dendrites forming independently in the matrix, indicating that some form of solute rejection has occurred. The intercellular regions are still amorphous at this stage, as shown by the ring diffraction patterns (Fig. 7c), presumably because they are enriched in boron and silicon, as is the residual glassy matrix.

An interesting result of our work is the observation that the cellular substructure of the surface crystals becomes progressively finer during growth. Even at the high growth rates associated with melt spinning, cell spacing is directly related to interface undercooling [19] and therefore the implication of this observation is that the crystal–melt interface temperature must be continuously decreasing during growth.

In most solidification processes, growth from undercooled melts would normally lead to an increase in interface temperature after nucleation due to the release of latent heat of fusion and this would result in a progressively coarser structure during growth. This effect has been reported many times for rapidly solidified fully crystalline alloys, for example in AlFe alloys [20], where the substructure often changes sharply from a very fine cellular morphology (zone A), to a significantly coarser cellular or dendritic morphology (zone B), during freezing. In rapid solidification of atomized droplets this transition has been associated with the point at which latent heat can no longer be entirely absorbed by conduction into the undercooled melt: heat must then be removed by the far less efficient process of convection to the surroundings. An identical structural change has also been reported in melt-spun ribbons of AlFe alloys [21] and a similar explanation for the zone A to zone B transition was offered, i.e. a change from the conduction of latent heat into the melt to conduction through the solidified layer after recalescence. It was noted that using a steel rather than a copper wheel for melt spinning resulted in fully zone A structures throughout the ribbon thickness and this was explained in terms of the higher heat removal rate obtained when using a steel wheel due to the more efficient wetting of the wheel surface by the melt. Under these conditions, it was suggested, the melt does not recalesce completely before the ribbon has completely solidified.

Although these results for fully crystalline alloys are consistent with the proposed heat transfer model, our results showing a progressive refinement of the cellular substructure as growth proceeds appear contradictory. Further consideration, however, suggests that a continually decreasing interface temperature is, in fact, a pre-requisite for a crystalline to glass transition, because once crystals have nucleated and begin to grow, glass can form subsequently only if the temperature of the melt ahead of the interface continues to fall towards the glass transition temperature, T_g. In order for this to happen, heat must be conducted away through the crystal and into the wheel faster than it is released as latent heat of fusion. Eventually, if the interface temperature reaches T_g, the crystal–melt interface will be "frozen-in" as a crystal–glass interface. This analysis is equivalent to Massalski and

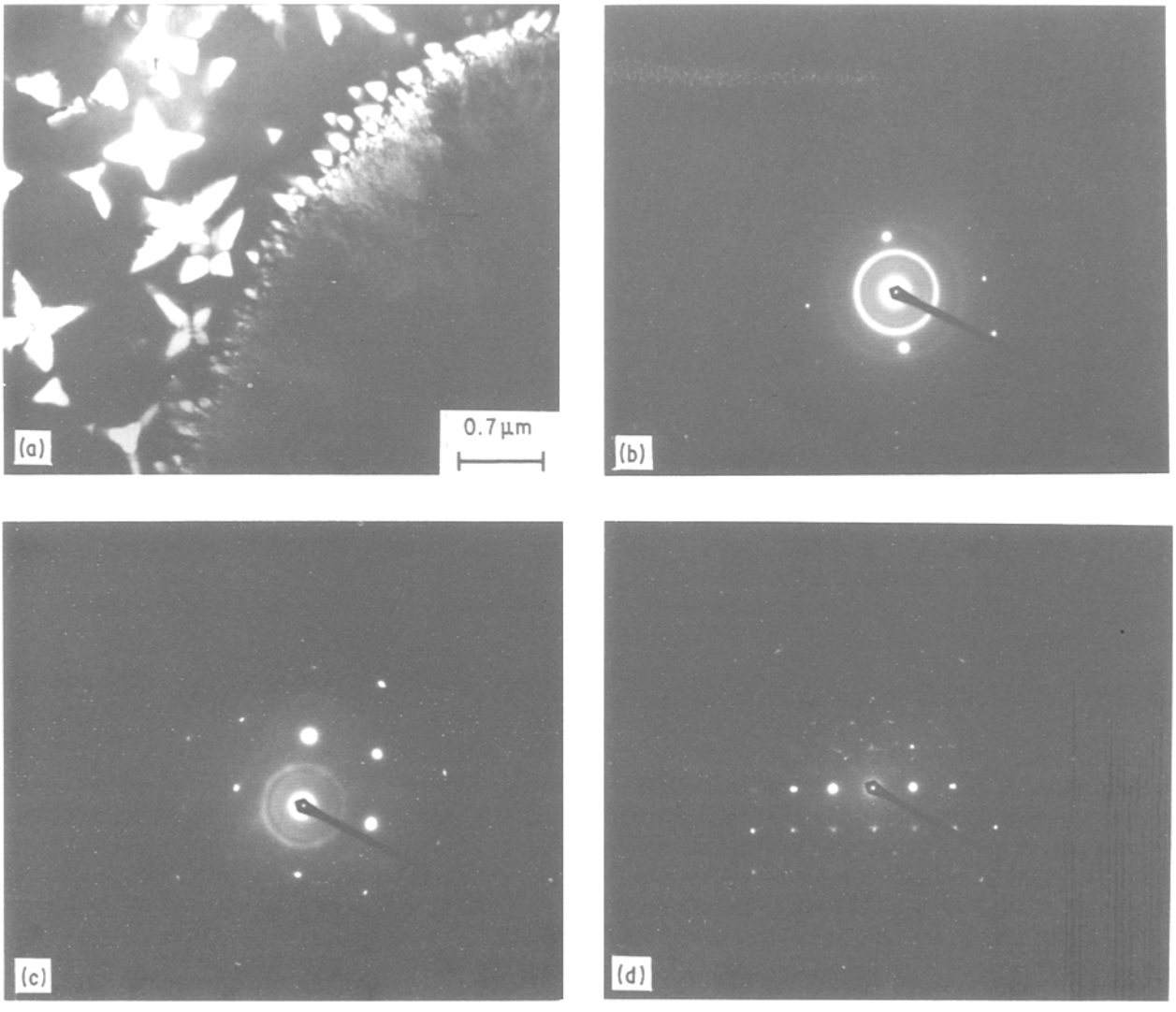

Figure 7 (a) Transmission electron photomicrograph of $Fe_{80}Si_{10}B_{10}$ heat treated to the first stage of crystallization showing nucleation and growth of α-Fe dendrites in the glassy matrix and the formation of dendritic perturbations on the substrate–crystal interface. (b) EDP from a dendrite in (a) and including the diffuse rings from the residual glassy matrix. (c) EDP from a substrate crystal, heat treated into the first stage of crystallization. The diffuse rings still persist in the pattern. (d) EDP from a substrate crystal, heat treated into the second stage of crystallization (fully transformed). The ring pattern has been replaced by diffraction spots.

Woychik's description of the transition occurring when the isotherms move through the melt faster than the crystals can grow. The fact that the substructure becomes finer during growth is evidence that the crystal-to-glass transition occurs, in these alloys at least, while the crystal growth rate is still increasing, contrary to Fredriksson's suggestion that the transition occurs after the growth rate has fallen to zero.

5. Conclusions

1. Wheel-side surface crystallization in metallic glass ribbons occurs preferentially at points on the wheel–puddle interface which are areas of high cooling rate and also probably active heterogeneous nucleation sites.

2. The crystals grow with a very fine cellular substructure with the intercellular regions freezing as metallic glass. The substructure becomes progressively finer during growth.

3. The crystal–glass transition can occur only when the crystal–melt interface temperature falls continuously to the glass transition temperature during growth. Thermal conditions during melt spinning must therefore be such that heat is removed by conduction into the wheel faster than it is released as latent heat at the interface.

References

1. L. A. DAVIS, N. DeCRISTOFARO and C. H. SMITH, in Proceedings of the Conference on Metallic Glasses: Science and Technology, Budapest, Hungary, 1980, p. 1.
2. M. MATSUURA, *J. Phys. F Met. Phys.* **15** (1985) 257.
3. *Idem*, in "Rapidly Solidified Materials", edited by P. W. Lee and R. S. Carbonara (ASM, Metals Park, Ohio, 1986) p. 261.
4. M. CHOI, D. M. DEASE, W. A. HINES, J. I. BUDNICK, G. H. HAYES and L. T. KABACOFF, *J. Appl. Phys.* **54** (1983) 4193.
5. G. A. JONES, S. F. H. PARKER, P. J. GRUNDY and D. G. LORD, *IEEE Trans. Mag.* **Mag 20** (1984) 1382.
6. H. FREDRIKSSON, A. OSTLUND and H. SODERHJELM, in "Proceedings of the 5th International Conference on Rapidly Quenched Metals", Wurzburg, 1985, edited by S. Steeb and H. Warlimont (Elsevier, Amsterdam, 1985) p. 187.
7. C. G. WOYCHIK, D. H. LOWNDES and T. B. MASSALSKI, *Acta Metall.* **33** (1985) 1861.

8. T. B. MASSALSKI and C. G. WOYCHIK, *ibid.* **33** (1985) 1873.
9. A. INOUE, M. KOMURO and T. MASUMOTO, *J. Mater. Sci.* **19** (1984) 4125.
10. N. DeCRISTOFARO, A. FREILICH and G. FISH, *ibid.* **17** (1982) 2365.
11. M. A. GIBSON and G. W. DELAMORE, to be published.
12. H. BILONI and B. CHALMERS, *Trans. AIME* **233** (1965) 373.
13. C. M. ADAM, in "Rapidly Solidified Amorphous and Crystalline Alloys", edited by B. H. Kear, B. C. Giessen and M. Cohen (Materials Research Society, Elsevier, New York, 1982) p. 411.
14. W. J. BOETTINGER, *ibid.*, p. 15.
15. T. F. KELLY and J. B. VANDERSANDE, in "Rapid Solidification Processing: Principles and Technologies 2" edited by R. Mehrabian, B. H. Kear and M. Cohen (Claitor's, Baton Rouge, Los Angeles 1980) p. 100.
16. W. J. BOETTINGER, L. BENDERSKY and J. G. EARLY, *Met. Trans. A* **17** (1986) 781.
17. M. C. M. FARQUAR, H. LIPSON and A. R. WEIL, *J. Iron Steel Inst.* **152** (1945) 457.
18. R. RAY and R. HASEGAWA, *Solid State Commun.* **27** (1978) 471.
19. C. G. LEVI and R. MEHRABIAN, *Met. Trans. A* **13** (1983) 13.
20. H. JONES, *Mater. Sci. Engng* **5** (1969/70) 1.
21. P. RENAUT and G. LAPASSET, in "Proceedings of the 5th International Conference on Rapidly Quenched Metals", Wurzburg, 1985, edited by S. Steeb and H. Warlimont (Elsevier, Amsterdam, 1985) p. 815.

Received 9 June
and accepted 20 August 1987